Field-Trial Quantum Key Distribution with Qubit-Based Frame Synchronization

Rui Guan, Jingchun Yu, Zhaoyun Li, Hongbo Xie, Yuxing Wei, Sen Li, Jing Wen, Xiaodong Liang, Yanwei Li, and Kejin Wei

Abstract—Quantum key distribution (QKD) is a cryptographic technique that uses quantum mechanical principles to enable secure key exchange, offering information-theoretic security guaranteed by physical laws. Practical deployment of QKD requires robust, cost-effective systems that can operate in challenging field environments. A major challenge is achieving reliable clock synchronization without adding hardware complexity. Conventional approaches often use separate classical light signals, which increase costs and introduce noise that degrades quantum channel performance. To address this limitation, we demonstrate a QKD system incorporating a recently proposed qubit-based distributed frame synchronization method, deployed over a metropolitan fiber network in Nanning, China. Using the polarization-encoded one-decoy-state BB84 protocol and the recently proposed qubit-based distributed frame synchronization method, our system achieves synchronization directly from the quantum signal, eliminating the need for dedicated synchronization hardware. Furthermore, to counteract dynamic polarization disturbances in urban fibers, the system integrates qubit-based polarization feedback control, enabling real-time polarization compensation through an automated polarization controller using data recovered from the qubit-based synchronization signals. During 12 hours of continuous operation, the system maintained a low average quantum bit error rate (QBER) of $1.12 \pm 0.48 \%$, achieving a secure key rate of 26.6 kbit/s under 18 dB channel loss. Even under a high channel loss of 40 dB, a finite-key secure rate of 115 bit/s was achieved. This study represents the first successful long-term validation of a frame-synchronizationbased QKD scheme in a real urban environment, demonstrating exceptional stability and high-loss tolerance, and offering an alternative for building practical, scalable, and cost-efficient quantum-secure communication networks.

Index Terms—Quantum key distribution, qubit-based synchronization, frame synchronization, in field.

I. INTRODUCTION

Quantum key distribution (QKD) is a cryptographic technique that leverages the fundamental principles of quantum

This study was supported by National Natural Science Foundation of China (Nos. 62171144 and 62031024), Guangxi Science Foundation (Nos. 2025GXNSFAA069137 and GXR-1BGQ2424005), and Innovation Project of Guangxi Graduate Education (No. YCBZ2025064). (Corresponding author: Xiaodong Liang, Yanwei Li, and Kejin Wei.)

Rui Guan, Jingchun Yu and Kejin Wei are with the Guangxi Key Laboratory for Relativistic Astrophysics, School of Physical Science and Technology, Guangxi University, Nanning 530004, China (kjwei@gxu.edu.cn).

Hongbo Xie, Yanwei Li is Ji Hua Laboratory, Foshan City, Guangdong Province, China.(yanwei201314@163.com)

Zhaoyun Li, Xiaodong Liang is the Guangxi Key Laboratory of Optical Network and Information Security, The 34th Research Institute of China Electronics Technology Group Corporation, Guilin 541004, Guangxi, China.(xdliang@bupt.cn)

Yuxing Wei, Sen Li, Jing Wen is Guangxi Zhuang Autonomous Region Information Center, Nanning 530201, China.

mechanics, such as the quantum no-cloning theorem and the uncertainty principle, to enable two remote parties to generate and share a secret key with information-theoretic security [1]. Since the introduction of the pioneering BB84 protocol in 1984, QKD has evolved from a theoretical concept into a practical technology [2]–[7], with significant potential to secure critical communications against current and future threats, including quantum computers.

Currently, most high-performance QKD systems operate in highly controlled laboratory environments [8]–[16], which differ substantially from real-world urban fiber networks. Transitioning QKD from controlled laboratory demonstrations to robust, cost-effective systems capable of operating in demanding real-world environments poses critical engineering challenges [17]–[29]. For wide deployment in existing telecommunications infrastructure, such as metropolitan fiber networks, QKD systems must maintain long-term stability despite environmental fluctuations, including temperature changes and physical fiber disturbances.

A key challenge in practical deployment is achieving high-precision clock synchronization between the communicating parties (Alice and Bob) without adding hardware complexity or cost [30]–[32]. Conventional approaches often use separate classical optical pulses transmitted over the same or parallel fiber [18], [22], [26], [33], [34]. However, this approach increases the system's component count and cost while introducing extraneous light that can generate noise [35]–[38], potentially reducing the sensitivity of single-photon detectors in the quantum channel and degrading overall system performance.

To address this limitation, qubit-based synchronization has been proposed [39]–[48]. This method derives synchronization signals directly from quantum states, eliminating the need for separate hardware and its associated drawbacks. A notable advancement is the qubit-based distributed frame synchronization method [45], which provides improved tolerance to channel attenuation, allowing the system to operate continuously without interruption. Its feasibility has been verified in laboratory environments [49]–[52]. However, the long-term stability and practical efficacy of this method had not been validated through extensive testing in dynamic urban fiber networks.

In this study, we demonstrate a QKD system incorporating a recently proposed qubit-based distributed frame synchronization method, deployed over a metropolitan fiber network in Nanning, China. Our system uses the polarization-encoded one-decoy-state BB84 protocol. By integrating qubit-based

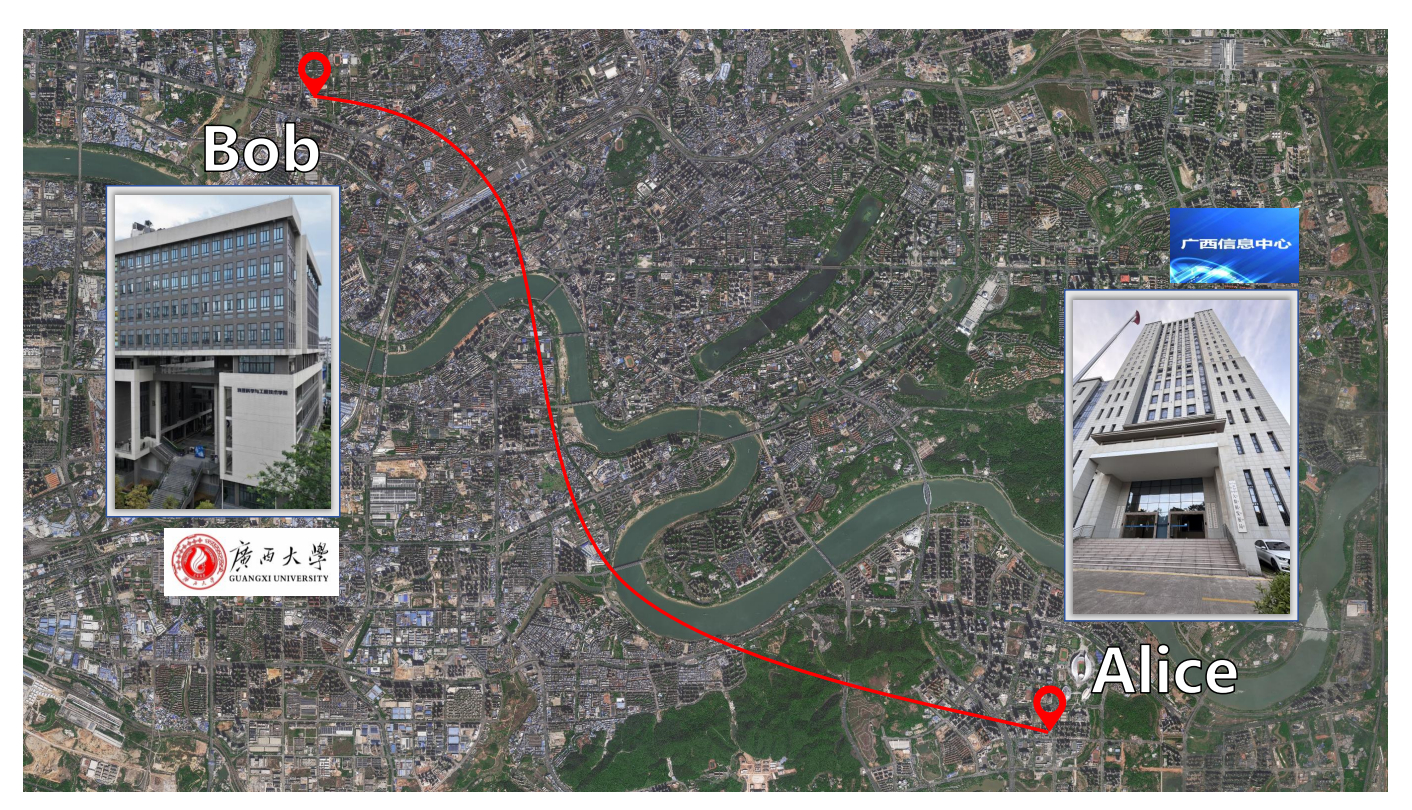


Fig. 1: Aerial view of the fiber link used in the QKD field trial performed in Nanning, China. [©2024 Baidu]. The link connects the transmitter (Alice), located at the Guangxi Zhuang Autonomous Region Information Center, with the receiver (Bob), situated at the School of Physical Science and Technology, Guangxi University.

polarization feedback control, the system actively compensates in real time for dynamic polarization disturbances in fielddeployed fibers using data recovered from the qubit-based synchronization signals.

Our experiments show that the system maintained a low average quantum bit error rate (QBER) of $1.12\pm0.48\%$ over 12 hours of continuous operation, achieving a secure key rate of 26.6 kbit/s under 18 dB channel loss. Even under a high channel loss of 40 dB, a finite-key secure rate of 115 bit/s was maintained. This study is the first successful long-term validation of a frame-synchronization-based QKD scheme in a real urban environment, demonstrating exceptional stability and high-loss tolerance. Our work provides a promising alternative for building practical, scalable, and cost-efficient quantum-secure communication networks.

The remainder of this paper is organized as follows. Section II describes the experimental setup in detail, Section III presents the results, and Section IV concludes the paper.

II. SETUP

Figure 1 illustrates aerial view of the experimental configuration, where the transmitter (Alice) is located at the Guangxi Zhuang Autonomous Region Information Center and the receiver (Bob) at the School of Physical Science and Technology, Guangxi University. The total measured link loss is approximately 18 dB. The fiber link withstands environmental disturbances as it traverses the Yongjiang River and the bustling urban area.

The used experimental setup is a polarization-encoding QKD setup, as shown in Figure 2. On the transmitter side (left panel of Figure 2), a commercial laser generates an optical pulse train with a repetition rate of 100 MHz and a wavelength of 1550 nm. This pulse train is first encoded by an intensity modulator to prepare two intensities of signals required for the one-decoy-state BB84 protocol. The intensity modulator employs a Sagnac interferometer configuration [53]–[55], consisting of a 50:50 polarization-maintaining beam splitter (PMBS), a lithium niobate phase modulator (PM), and a 1 m polarization-maintaining fiber (PMF) delay line. Following intensity modulation, the optical pulses are immediately coupled into a Sagnac-based polarization modulator (Sagnac-POL) module for qubit polarization encoding. The core component of this module is a custom polarization beam splitter (CPM) based on a Sagnac interferometer configuration and a PM. A crucial design aspect is the precise alignment of the CPM's polarization-maintaining fiber input axis at a 45° angle relative to the principal axes of the beam splitter. This alignment enables efficient splitting of incident pulses into two orthogonally polarized components. By applying a pre-calibrated voltage signal from the RF output port on the 100 MHz board to the PM within the Sagnac-POL, we prepare the four BB84 polarization states as follows:

$$|\psi\rangle = \frac{|H\rangle + e^{i\theta} |V\rangle}{\sqrt{2}}, \quad \theta \in \left\{0, \frac{\pi}{2}, \pi, \frac{3\pi}{2}\right\}$$
 (1)

where θ denotes the applied phase and $\theta \in \{0, \pi\}$ ($\theta \in$

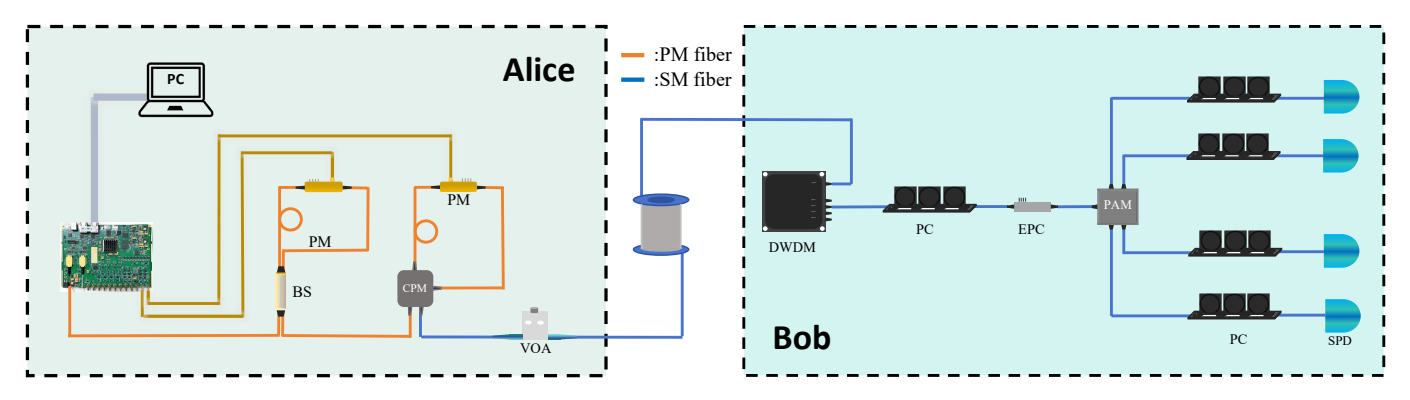


Fig. 2: Schematic representation of the setup employed in the experiment. In the upper-left and upper-right boxes we represent the setup for the transmitter(Alice) and receiver(Bob), respectively. BS, beam splitter; PM, phase modulator; CPM, customized polarization module; VOA, variable optical attenuator; DWDM, dense wavelength division multiplexing; EPC, electronic polarization controller; PAM, polarization analysis module; SPD, single photon detector; PM fiber, polarization-maintaining fiber; SM fiber, single mode fiber.

 $\left\{\frac{\pi}{2}, \frac{3\pi}{2}\right\}$) corresponds to the states in the Z (X) basis.

Subsequently, the polarization-modulated light exits from the CPM's output port, is attenuated to the single-photon regime by variable optical attenuator (VOA), and is transmitted over the quantum channel.

At the receiver (Bob), a dense wavelength division multiplexing (DWDM) filter suppresses dark count increases caused by light leakage and imperfect isolation in the field-deployed fiber link. An electrically controlled polarization controller (EPC) then aligns the incoming polarization states with the measurement basis. Photon detection is achieved using four commercial superconducting nanowire single-photon detectors (SNSPDs, Photon Technology Co., Ltd.). The detectors operate at 2.1 K, with a detection efficiency of approximately 60 %, a dead time of 40 ns, a timing jitter of \leq 70 ps, and a dark count rate of about 40 Hz. Detection events are recorded using a high-speed time-to-digital converter (TDC, TimeTagger20, Swabian Instruments) and transmitted to Bob's computer for time synchronization and polarization drift compensation.

The time recovery employs the distributed frame synchronization technique proposed in [45], which reconstructs the clock cycle from event detection without relying on any external reference signal. A brief overview of this method is provided below. Specifically, Alice generates a correlation code S^A of length L and divides it into L single-qubit segments. Each segment is concatenated with M random qubits to form a composite qubit sequence, which is then transmitted to Bob through a lossy quantum channel. Upon receiving the qubit sequence, Bob performs period recovery, time compensation, and time offset estimation based on the detected qubit data.

To compensate for polarization drift in the deployed fiber channel caused by environmental disturbances, we employ a qubit-based polarization compensation method that uses a shared quantum bit sequence between the communicating parties to enable dynamic polarization control. The procedure is as follows: after Bob completes time synchronization, the QBER in the Z and X bases is calculated from the disclosed quantum bit sequence. The estimated QBER is then fed into

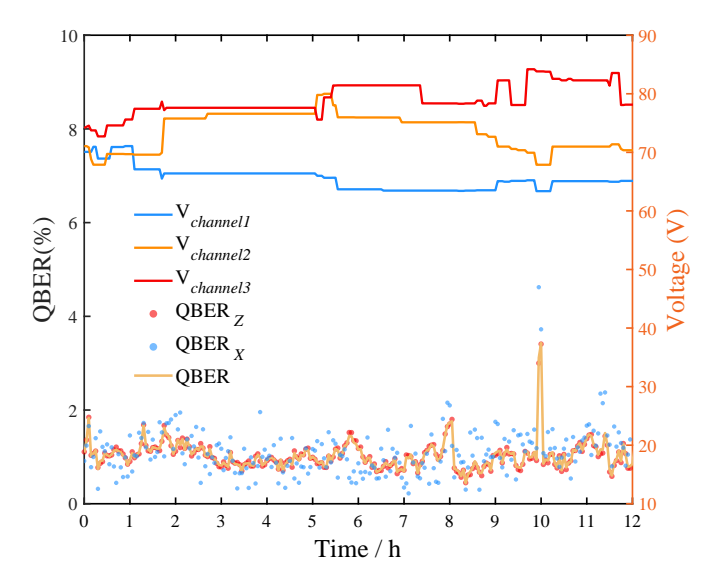


Fig. 3: QBER on Z(X) basis of the system (left axis) and the feedback voltage of EPC (right axis, for EPC channels 1, 2, and 3 in blue, purple, and orange) over a 12-hour continuous operation in a field-deployed fiber link with 18 dB channel loss. The red (blue) point denotes the quantum bit error in Z(X) basis, which are recorded every 2.5 minutes.

a gradient descent optimization algorithm running on Bob's computer, which adjusts the EPC driving voltage in real time to minimize the QBER. This process iterates until the estimated QBER falls below a predefined threshold.

III. EXPERIMENTAL RESULTS

We first evaluate the long-term stability of the QBER and the performance of real-time polarization feedback control. As shown in Figure 3, we recorded the real-time QBER and corresponding feedback voltage of the EPC during a 12-hour continuous operation over a field-deployed fiber link with a channel loss of 18 dB. The feedback voltage of the EPC was adjusted in real time, and the QBER exhibited minor

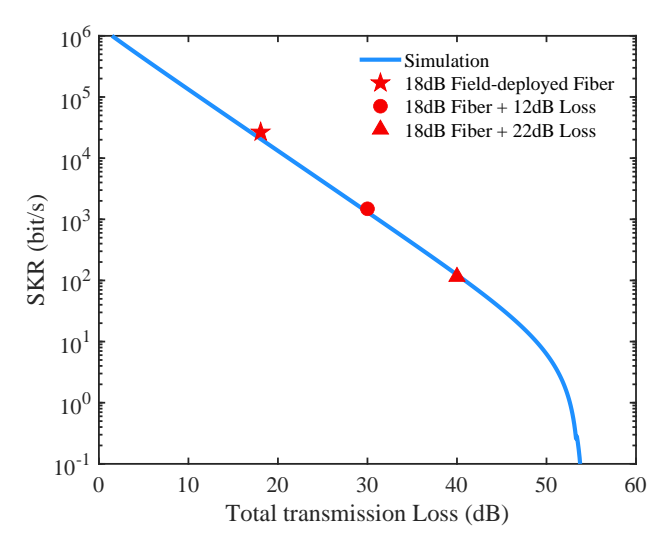


Fig. 4: The secure key rate under different transmission losses. The blue line shows the simulation results based on our experimental parameters, the red stars represent the experimental results obtained over real fiber links. The red circle and triangle markers denote the results measured over the same field fiber with additional 12 dB and 22 dB losses emulated by VOA, corresponding to total losses of 30 dB and 40 dB, respectively.

fluctuations due to environmental disturbances such as temperature variations and mechanical stress in the metropolitan fiber network. Despite these disturbances, the system maintained an exceptionally low average QBER. An average QBER $_Z$ is measured to be $1.12\pm0.51\%$ for the Z basis, while for X basis, the average QBER $_X$ is $1.10\pm0.51\%$. The total QBER for both two bases is $1.12\pm0.48\%$, demonstrating the robustness of the proposed qubit-based synchronization and polarization compensation method.

We further evaluate the secure key rate under various transmission loss conditions. The experiment was first conducted over a deployed fiber link with an optical loss of approximately 18 dB. To assess performance over longer distances, VOA was used to emulate higher channel losses of 30 dB and 40 dB. For link losses of 18 dB and 30 dB, the total length of the periodic correlation code was set to L, and the ratio M was configured as 7:1. Under the 40 dB loss condition, the ratio M was adjusted to 3:1 to increase the number of synchronization sequences and reduce the risk of synchronization failure caused by excessive attenuation of the synchronization signal. For each distance, approximately 10⁷ detection events were accumulated. Before each estimation, a full optimization of the implementation parameters for the one-decoy-state protocol was performed to ensure optimal system performance [56]. For instance, in the 18 dB experimental scenario, the signal and decoy state intensities were set to $\mu = 0.565$ and $\nu = 0.143$, respectively, while the probabilities of sending the signal state and selecting the Z basis were $p_{\mu} = 0.798$ and $p_{\rm Z} = 0.944$. On Bob's side, the probabilities of selecting the Z and X bases were fixed and equal.

The finite-key analysis was performed using the method described in [57], and the final secure key rate was estimated

using the following formula:

$$R = \left(s_{z,0}^L + s_{z,1}^L \left(1 - h(e_{z,1}^{ph})\right) - \lambda_{EC} - 6\log_2\frac{19}{\epsilon_{sec}} - \log_2\frac{2}{\epsilon_{cor}}\right) \cdot \frac{q \cdot f}{N}$$
(2)

Here, $s_{z,0}^L$ denotes the lower bound of detection events that Bob receives when Alice sends a vacuum state in the Z basis. $s_{z,1}^L$ denotes the lower bound of single-photon detection events in the Z basis, assuming that Alice sends only single-photon states. $e_{z,1}^{ph}$ represents the upper bound of the phase error rate for single-photon events. $\lambda_{EC} = n_z f_e h(e_z)$ denotes the number of bits consumed during error correction, where e_z is the quantum bit error rate (QBER) and $f_e = 1.16$ is the error correction efficiency factor. ϵ_{sec} and ϵ_{cor} are security and correctness parameters, respectively. The binary entropy function is defined as $h(x) = -x \log_2(x) - (1-x) \log_2(1-x)$. f is the system repetition frequency, and N denotes the total number of optical pulses, including both synchronization and random pulses. q = M/(M+1) denotes the fraction of signals used for key distribution.

The experimental results are presented in Figure 4, and the corresponding parameters and performance metrics are summarized in Table I. The results clearly demonstrate that the system sustains a high secure key rate (SKR) of 26.6 kbit/s over the deployed fiber link in Nanning. Even under extreme channel attenuations of 30 dB and 40 dB—emulated using VOA—the system achieves finite-key secure rates of 1.48 kbit/s and 115 bit/s, respectively. These findings exhibit strong agreement with theoretical predictions, confirming the robustness and efficiency of the qubit-based synchronization and polarization control mechanisms under high-loss conditions.

IV. CONCLUSION

This study successfully demonstrates the long-term stability and robustness of a qubit-based distributed frame synchronization QKD system deployed over a real-world metropolitan fiber network. By integrating polarization feedback control and qubit-based synchronization, the system achieves stable synchronization and real-time polarization compensation without the need for external classical channels or additional hardware. Experimental results confirm its excellent performance under challenging conditions: during 12 hours of continuous operation, the system maintained an average QBER of $1.12 \pm 0.48 \%$ at 18 dB channel loss, while achieving a secure key rate of 26.6 kbit/s. Even under extreme attenuation of 40 dB, the system sustained a finite-key secure rate of 115 bit/s, demonstrating remarkable tolerance to high channel loss. These findings underscore the practicality and field readiness of qubit-based synchronization for real-world QKD deployments, where environmental fluctuations are unavoidable.

REFERENCES

 C. H. Bennett and G. Brassard, "Quantum cryptography: Public key distribution and coin tossing," *International Conference on Computers*, Systems and Signal Processing, Bangalore, India, Dec 9-12, 1984, pp. 175–179, 1984.

TABLE I: Experimental parameters and results. L and Loss are the channel lengths and channel losses, respectively. μ (ν) is the intensity of the signal (decoy) state, P_z (P_x) is the probability of choosing Z (X) basis, n_z is the amount of data accumulated on the Z basis, t is the total accumulated time of measurement, Ratio denotes the ratio between the number of qubits for synchronization and that of random polarization states of four BB84 polarizations. τ_b is the period measured by Bob, $n_{z,\mu}$ ($n_{x,\mu}$) is the raw count measured under Z (X) basis for the signal state, $n_{z,\nu}$ ($n_{x,\nu}$) is the raw count measured for the decoy state under Z (X) basis, $m_{z,\mu}$ ($m_{x,\mu}$) is the error count measured under Z (X) basis for the signal state, $m_{z,\nu}$ ($m_{x,\nu}$) is the error count measured for the decoy state under Z (X) basis, QBER $_z$ is quantum bit error rates of Z basis, ϕ_z^U is the upper bound of phase error rate, $s_{z,1}^L$ is the lower bound for measuring single-photon events in the Z-basis, l is the secret key length, and SKR is the final secure key rate.

$L \; (\mathrm{km})$	Loss (dB)	μ	ν	P_{μ}	P_{ν}	P_z	P_x	Ratio) 1	n_z	t (s)	τ_b (ns)		$QBER_z$
90	18.07	0.466	0.127	0.761	0.239	0.935	0.065	1:7	99	21 359	145.5	$10.0 \pm 8.8 \times 1$	0^{-8}	0.925
150	30	0.465	0.126	0.761	0.239	0.934	0.066	1:7	98	44 391	2271.9	$10.0 \pm 3.2 \times 1$	0^{-7}	1.134
200	40	0.464	0.125	0.761	0.239	0.931	0.069	1:3	98	98 948	22 779.7	$10.0 \pm 1.8 \times 1$	0^{-7}	1.749
L (km)	$n_{z,\mu}$	$m_{z,\mu}$	$n_{x,\mu}$	$m_{x,\mu}$	$n_{z,\nu}$	\overline{m}	z, ν r	dx, ν	$m_{x, u}$	ϕ_z^U	$s_{z,1}^L$	l	SKR ((bit/s)
90	9 157 392	84 469	735 824	6302	763 96	7 72	293 61	775	762	0.0227	5 620 092	3 868 037	2.66 >	< 10 ⁴
150	9 086 317	102 679	730 681	9157	758 07	4 89	019 61	348	1151	0.0323	5 533 409	3 370 711	1.48 >	< 10 ³
200	9115411	150 978	766 631	15 029	783 53	7 22 1	14 68	3 149	1969	0.0443	5 528 936	2 622 953	1.15 >	$< 10^2$

- [2] A. Orieux and E. Diamanti, "Recent advances on integrated quantum communications," J. Opt., vol. 18, no. 8, Aug 2016.
- [3] S. Pirandola, U. L. Andersen, L. Banchi, M. Berta, D. Bunandar, R. Colbeck, D. Englund, T. Gehring, C. Lupo, C. Ottaviani, J. L. Pereira, M. Razavi, J. S. Shaari, M. Tomamichel, V. C. Usenko, G. Vallone, P. Villoresi, and P. Wallden, "Advances in quantum cryptography," Adv. Opt. Photon., vol. 12, no. 4, pp. 1012–1236, Dec 2020.
- [4] F. Xu, X. Ma, Q. Zhang, H.-K. Lo, and J.-W. Pan, "Secure quantum key distribution with realistic devices," *Rev. Mod. Phys.*, vol. 92, no. 2, p. 025002, 2020.
- [5] Q. Liu, Y. Huang, Y. Du, Z. Zhao, M. Geng, Z. Zhang, and K. Wei, "Advances in chip-based quantum key distribution," *Entropy*, vol. 24, no. 10, p. 1334, 2022.
- [6] Y. Cao, Y. Zhao, Q. Wang, J. Zhang, S. X. Ng, and L. Hanzo, "The evolution of quantum key distribution networks: On the road to the qinternet," *IEEE Commun. Surv. Tut.*, vol. 24, no. 2, pp. 839–894, 2022.
- [7] G. Granados, W. Velasquez, R. Cajo, and M. Antonieta-Alvarez, "Quantum key distribution in multiple fiber networks and its application in urban communications: A comprehensive review," *IEEE Access*, vol. 13, pp. 100446–100461, 2025.
- [8] A. Boaron, G. Boso, D. Rusca, C. Vulliez, C. Autebert, M. Caloz, M. Perrenoud, G. Gras, F. Bussières, M.-J. Li, D. Nolan, A. Martin, and H. Zbinden, "Secure quantum key distribution over 421 km of optical fiber," *Phys. Rev. Lett.*, vol. 121, p. 190502, Nov 2018.
- [9] F. Grünenfelder, A. Boaron, D. Rusca, A. Martin, and H. Zbinden, "Performance and security of 5 ghz repetition rate polarization-based quantum key distribution," *Appl. Phys. Lett.*, vol. 117, no. 14, 2020.
- [10] K. Wei, W. Li, H. Tan, Y. Li, H. Min, W.-J. Zhang, H. Li, L. You, Z. Wang, X. Jiang, T.-Y. Chen, S.-K. Liao, C.-Z. Peng, F. Xu, and J.-W. Pan, "High-speed measurement-device-independent quantum key distribution with integrated silicon photonics," *Phys. Rev. X*, vol. 10, p. 031030, Aug 2020.
- [11] T. K. Paraiso, T. Roger, D. G. Marangon, I. De Marco, M. Sanzaro, R. I. Woodward, J. F. Dynes, Z. Yuan, and A. J. Shields, "A photonic integrated quantum secure communication system," *Nat. Photon.*, vol. 15, no. 11, pp. 850–856, 2021.
- [12] L. Zhou, J. Lin, Y. Jing, and Z. Yuan, "Twin-field quantum key distribution without optical frequency dissemination," *Nat. Commun.*, vol. 14, no. 1, p. 928, 2023.
- [13] F. Grünenfelder, A. Boaron, G. V. Resta, M. Perrenoud, D. Rusca, C. Barreiro, R. Houlmann, R. Sax, L. Stasi, S. El-Khoury *et al.*, "Fast single-photon detectors and real-time key distillation enable high secretkey-rate quantum key distribution systems," *Nat. Photon.*, vol. 17, no. 5, pp. 422–426, 2023.
- [14] W. Li, L. Zhang, H. Tan, Y. Lu, S.-K. Liao, J. Huang, H. Li, Z. Wang, H.-K. Mao, B. Yan *et al.*, "High-rate quantum key distribution exceeding 110 mb s–1," *Nat. Photon.*, vol. 17, no. 5, pp. 416–421, 2023.
- [15] Y. Liu, W.-J. Zhang, C. Jiang, J.-P. Chen, C. Zhang, W.-X. Pan, D. Ma, H. Dong, J.-M. Xiong, C.-J. Zhang, H. Li, R.-C. Wang, J. Wu, T.-Y. Chen, L. You, X.-B. Wang, Q. Zhang, and J.-W. Pan, "Experimental

- twin-field quantum key distribution over 1000 km fiber distance," *Phys. Rev. Lett.*, vol. 130, p. 210801, May 2023.
- [16] Z. Chen, X. Wang, S. Yu, Z. Li, and H. Guo, "Continuous-mode quantum key distribution with digital signal processing," *npj Quant. Inf.*, vol. 9, no. 1, p. 28, 2023.
- [17] E. Diamanti, H.-K. Lo, B. Qi, and Z. Yuan, "Practical challenges in quantum key distribution," npj Quant. Inf., vol. 2, Nov 8 2016.
- [18] D. Bacco, I. Vagniluca, B. Da Lio, N. Biagi, A. Della Frera, D. Calonico, C. Toninelli, F. S. Cataliotti, M. Bellini, L. K. Oxenlowe, and A. Zavatta, "Field trial of a three-state quantum key distribution scheme in the florence metropolitan area," *EPJ Quantum Technol.*, vol. 6, no. 1, Oct 28 2019.
- [19] H. Liu, C. Jiang, H.-T. Zhu, M. Zou, Z.-W. Yu, X.-L. Hu, H. Xu, S. Ma, Z. Han, J.-P. Chen, Y. Dai, S.-B. Tang, W. Zhang, H. Li, L. You, Z. Wang, Y. Hua, H. Hu, H. Zhang, F. Zhou, Q. Zhang, X.-B. Wang, T.-Y. Chen, and J.-W. Pan, "Field test of twin-field quantum key distribution through sending-or-not-sending over 428 km," *Phys. Rev. Lett.*, vol. 126, p. 250502, Jun 2021.
- [20] J.-P. Chen, C. Zhang, Y. Liu, C. Jiang, D.-F. Zhao, W.-J. Zhang, F.-X. Chen, H. Li, L.-X. You, Z. Wang, Y. Chen, X.-B. Wang, Q. Zhang, and J.-W. Pan, "Quantum key distribution over 658 km fiber with distributed vibration sensing," *Phys. Rev. Lett.*, vol. 128, p. 180502, May 2022.
- [21] M. Stanley, Y. Gui, D. Unnikrishnan, S. Hall, and I. Fatadin, "Recent progress in quantum key distribution network deployments and standards," J. Phys. Conf. Ser., vol. 2416, no. 1, p. 012001, Dec 2022.
- [22] W. Li, L. Zhang, Y. Lu, Z.-P. Li, C. Jiang, Y. Liu, J. Huang, H. Li, Z. Wang, X.-B. Wang, Q. Zhang, L. You, F. Xu, and J.-W. Pan, "Twinfield quantum key distribution without phase locking," *Phys. Rev. Lett.*, vol. 130, p. 250802, Jun 2023.
- [23] Y.-C. Kao, S.-H. Huang, C.-H. Chang, C.-H. Wu, S.-H. Chu, J. Jiang, A.-C. Zhang, S.-Y. Huang, J.-H. Yan, K.-M. Feng, and C.-S. Chuu, "Field test of quantum key distribution with high key creation efficiency," *Opt. Express*, vol. 31, no. 19, pp. 30 239–30 247, Sep 2023.
- [24] Y.-L. Tang, Z.-L. Xie, C. Zhou, D. Zhang, M.-L. Xu, J. Sun, D. Sun, Y.-X. Xu, L.-W. Wang, Y. Ma, Y.-K. Zhao, M.-S. Jiang, Y. Wang, J. Li, K. Xue, N. Yu, M.-S. Zhao, D.-D. Li, W.-S. Bao, and S.-B. Tang, "Field test of quantum key distribution over aerial fiber based on simple and stable modulation," *Opt. Express*, vol. 31, no. 16, pp. 26301–26313, Jul 31 2023.
- [25] G. Bertaina, C. Clivati, S. Donadello, C. Liorni, A. Meda, S. Virzi, M. Gramegna, M. Genovese, F. Levi, D. Calonico, M. Dispenza, and I. P. Degiovanni, "Phase noise in real-world twin-field quantum key distribution," Adv. Quantum Technol., vol. 7, no. 6, Jun 2024.
- [26] L. Zhou, J. Lin, C. Ge, Y. Fan, Z. Yuan, H. Dong, Y. Liu, D. Ma, J.-P. Chen, C. Jiang, X.-B. Wang, L.-X. You, Q. Zhang, and J.-W. Pan, "Independent-optical-frequency-comb-powered 546-km field test of twin-field quantum key distribution," *Phys. Rev. Appl.*, vol. 22, p. 064057, Dec 2024.
- [27] Z. Li, T. Dou, M. Cheng, Y. Liu, and J. Tang, "Field experimental mode-

- pairing quantum key distribution with intensity fluctuations," *Opt. Lett.*, vol. 49, no. 23, pp. 6609–6612, Dec 2024.
- [28] H.-T. Zhu, Y. Huang, W.-X. Pan, C.-W. Zhou, J. Tang, H. He, M. Cheng, X. Jin, M. Zou, S. Tang, X. Ma, T.-Y. Chen, and J.-W. Pan, "Field test of mode-pairing quantum key distribution," *Optica*, vol. 11, no. 6, pp. 883–888, Jun 2024.
- [29] F. Picciariello, I. Karakosta-Amarantidou, E. Rossi, M. Avesani, G. Foletto, L. Calderaro, G. Vallone, P. Villoresi, and F. Vedovato, "Intermodal quantum key distribution field trial with active switching between fiber and free-space channels," EPJ Quantum Technol., vol. 12, no. 1, Dec 2025.
- [30] A. Pljonkin, K. Rumyantsev, and P. K. Singh, "Synchronization in quantum key distribution systems," *Cryptography*, vol. 1, no. 3, 2017.
- [31] A. Meda, A. Mura, S. Virzì, A. Avella, F. Levi, I. P. Degiovanni, A. Geraldi, M. Valeri, S. Di Bartolo, T. Catuogno et al., "Qkd protected fiber-based infrastructure for time dissemination," Sci. Rep., vol. 15, no. 1, p. 13419, 2025.
- [32] J. Krause, N. Walenta, J. Hilt, and R. Freund, "Clock-offset recovery with sublinear complexity enables synchronization on low-level hardware for quantum key distribution," *Phys. Rev. Appl.*, vol. 23, p. 044015, Apr 2025.
- [33] J.-P. Chen, C. Zhang, Y. Liu, C. Jiang, W.-J. Zhang, Z.-Y. Han, S.-Z. Ma, X.-L. Hu, Y.-H. Li, H. Liu, F. Zhou, H.-F. Jiang, T.-Y. Chen, H. Li, L.-X. You, Z. Wang, X.-B. Wang, Q. Zhang, and J.-W. Pan, "Twinfield quantum key distribution over a 511km optical fibre linking two distant metropolitan areas," *Nat. Photon.*, vol. 15, no. 8, pp. 570–575, Aug 2021.
- [34] N. Chandra and P. K. Krishnamurthy, "Fpga-based synchronization of frequency-domain interferometer for qkd," *IEEE Transactions on Quantum Engineering*, vol. 6, no. 4100111, pp. 1–10, 2025.
- [35] T. F. da Silva, G. B. Xavier, G. P. Temporao, and J. P. von der Weid, "Impact of raman scattered noise from multiple telecom channels on fiber-optic quantum key distribution systems," *J. Lightwave. Technol.*, vol. 32, no. 13, pp. 2332–2339, Jul 1 2014.
- [36] S. Aleksic, F. Hipp, D. Winkler, A. Poppe, B. Schrenk, and G. Franzl, "Perspectives and limitations of qkd integration in metropolitan area networks," *Opt. Express*, vol. 23, no. 8, pp. 10359–10373, Apr 202015.
- [37] I. A. Burenkov, A. Semionov, Hala, T. Gerrits, A. Rahmouni, D. Anand, Y.-S. Li-Baboud, O. Slattery, A. Battou, and S. V. Polyakov, "Synchronization and coexistence in quantum networks," *Opt. Express*, vol. 31, no. 7, pp. 11431–11446, Mar 2023.
- [38] A. Ramesh, D. R. Reilly, K. F. Lee, P. M. Moraw, J. Chung, M. S. Islam, C. Pena, X. Han, R. Kettimuthu, P. Kumar, and G. S. Kanter, "Hong-ou-mandel interference with a coexisting clock using transceivers for synchronization over deployed fiber," *Opt. Commun.*, vol. 576, Mar 2025.
- [39] L. Calderaro, A. Stanco, C. Agnesi, M. Avesani, D. Dequal, P. Villoresi, and G. Vallone, "Fast and simple qubit-based synchronization for quantum key distribution," *Phys. Rev. Appl.*, vol. 13, p. 054041, May 2020.
- [40] C. Agnesi, M. Avesani, L. Calderaro, A. Stanco, G. Foletto, M. Zahidy, A. Scriminich, F. Vedovato, G. Vallone, and P. Villoresi, "Simple quantum key distribution with qubit-based synchronization and a selfcompensating polarization encoder," *Optica*, vol. 7, no. 4, pp. 284–290, Apr 2020.
- [41] M. Avesani, L. Calderaro, G. Foletto, C. Agnesi, F. Picciariello, F. B. L. Santagiustina, A. Scriminich, A. Stanco, F. Vedovato, M. Zahidy, G. Vallone, and P. Villoresi, "Resource-effective quantum key distribution: a field trial in padua city center," *Opt. Lett.*, vol. 46, no. 12, pp. 2848–2851, Jun 15 2021.
- [42] R. D. Cochran and D. J. Gauthier, "Qubit-based clock synchronization for qkd systems using a bayesian approach," *Entropy*, vol. 23, no. 8, Aug 2021.
- [43] D. Scalcon, C. Agnesi, M. Avesani, L. Calderaro, G. Foletto, A. Stanco, G. Vallone, and P. Villoresi, "Cross-encoded quantum key distribution exploiting time-bin and polarization states with qubit-based synchronization," Adv. Quantum Technol., vol. 5, no. 12, Dec 2022.
- [44] N. S. Azahari, N. Z. Harun, C. Chai Wen, S. N. Ramli, and Z. Ahmad Zukarnain, "Review of clock synchronization in quantum communications," in *Proceedings of the 2024 13th International Conference on Software and Computer Applications*, ser. ICSCA '24. New York, NY, USA: Association for Computing Machinery, 2024, p. 350–356.
- [45] Y. Chen, C. Huang, G. Lin, S. Huang, Z. Zhang, and K. Wei, "Qubit-based distributed frame synchronization for quantum key distribution," J. Lightwave. Technol., vol. 43, no. 11, pp. 5032–5039, 2025.
- [46] Z.-K. Huang, J.-X. Li, F.-Y. Lu, Z.-H. Wang, S. Wang, Z.-Q. Yin, D.-Y. He, W. Chen, G.-C. Guo, and Z.-F. Han, "Qubit-based synchronization

- algorithm for measurement-device-independent quantum key distribution," *J. Lightwave. Technol.*, vol. 43, no. 7, pp. 3041–3050, Apr 1 2025.
- [47] H.-B. Sun, J. Li, X.-W. Chu, J.-Y. Liu, H.-J. Ding, and Q. Wang, "Optimized qubit-based synchronization in quantum key distribution," *IEEE Commun. Lett.*, vol. 29, no. 5, pp. 1087–1091, 2025.
- [48] F.-Y. Lu, Z.-K. Huang, J.-J. Deng, C. Zhang, S. Wang, D.-Y. He, Z.-Q. Yin, W. Chen, G.-C. Guo, and Z.-F. Han, "Fast qubit-based frequency recovery algorithm for quantum key distribution," arXiv preprint arXiv:2509.17849, 2025.
- [49] K. Wei, X. Hu, Y. Du, X. Hua, Z. Zhao, Y. Chen, C. Huang, and X. Xiao, "Resource-efficient quantum key distribution with integrated silicon photonics," *Photon. Res.*, vol. 11, no. 8, pp. 1364–1372, Aug 2023
- [50] C. Huang, Y. Chen, T. Luo, W. He, X. Liu, Z. Zhang, and K. Wei, "A cost-efficient quantum access network with qubit-based synchronization," Sci. China-Phys. Mech. Astron., vol. 67, no. 4, p. 240312, 2024.
- [51] W. Chen, "Breaking the synchronization barrier: Machine learningenhanced qubit-based synchronization enables 200 km self-synchronized rfi-qkd," Sci. China-Phys. Mech. Astron., vol. 68, no. 7, p. 270332, 2025.
- [52] Z. Tian, Z. Xie, Y. Chen, X. Fan, J. Huang, T. Mu, J. Guo, K. Wei, and S. Sun, "Reference-frame-independent quantum key distribution based on machine-learning-enhanced qubit-based synchronization," Sci. China-Phys. Mech. Astron., vol. 68, no. 7, p. 270312, 2025.
- [53] D. Ma, X. Liu, C. Huang, H. Chen, H. Lin, and K. Wei, "Simple quantum key distribution using a stable transmitter-receiver scheme," *Opt. Lett.*, vol. 46, no. 9, pp. 2152–2155, May 2021.
- [54] C. Agnesi, M. Avesani, A. Stanco, P. Villoresi, and G. Vallone, "All-fiber self-compensating polarization encoder for quantum key distribution," Opt. Lett., vol. 44, no. 10, pp. 2398–2401, May 2019.
- [55] G. L. Roberts, M. Pittaluga, M. Minder, M. Lucamarini, J. F. Dynes, Z. L. Yuan, and A. J. Shields, "Patterning-effect mitigating intensity modulator for secure decoy-state quantum key distribution," *Opt. Lett.*, vol. 43, no. 20, pp. 5110–5113, Oct 2018.
- [56] Z. Li and K. Wei, "Improving Parameter Optimization in Decoy-State Quantum Key Distribution," *Quantum Eng.*, vol. 2022, p. 9717591, 2022.
- 57] D. Rusca, A. Boaron, F. Grünenfelder, A. Martin, and H. Zbinden, "Finite-key analysis for the 1-decoy state qkd protocol," *Appl. Phys. Lett.*, vol. 112, no. 17, 2018.